EMSL Research Highlights

Laser and Electrical Current Induced Phase Transformation of In_2Se_3 Semiconductor Thin Film on Si(111)

CY Lu,[a] PJ Shamberger, [a] EN Yitamben, [a] KM Beck,[b] AG Joly,[c] MA Olmstead,[a] and FS Ohuchi[a]
(a) University of Washington, Seattle, Washington
(b) EMSL, Richland, Washington
(c) Pacific Northwest National Laboratory, Richland, Washington

Materials with rapid and reversible switching between amorphous and crystalline phases, and which exhibit significant electrical resistivity or optical reflectivity change between these phases, are promising candidates for phase-change non-volatile memory. The strong change in optical reflectivity during the amorphous-crystalline phase transition is the basis of re-writeable compact disk and digital video disk technology. During the past decade, binary chalcogenide semiconductors such as InSe/GaSe and In_2Se_3 have been investigated as potential phase-change media in proposed data storage and memory devices. This research investigates the phase-change mechanisms of In_2Se_3 using EMSL's photoemission electron microscope capability. This research will be highlighted in a journal article published this summer in Applied Physics A.

The electrical resistivity of In_2Se_3 increases by a factor of 10^5 from the crystalline to the amorphous state. However, the structural details of phase-change in In_2Se_3 films on silicon and the energetic requirements for phase change have not been fully explored. In_2Se_3 exhibits a complex phase system in which various structures with different arrangements of inherent defects can form. This complexity originates from many energetically similar routes by which trivalent and divalent atoms can combine to satisfy their bonding requirements and leads to several crystalline phases with the same In_2Se_3 stoichiometry.

This research analyzes the crystallization and amorphization of In_2Se_3 thin films on Si(111) (~ 30 nm thick) via resistive heating and laser annealing, respectively. The initially amorphous films were crystallized using resistive heating (time-scale of several seconds), while a 150-micron-diameter spot was re-amorphized using nanosecond laser annealing. The film morphology and conductivity were probed with scanning tunneling microscopy and

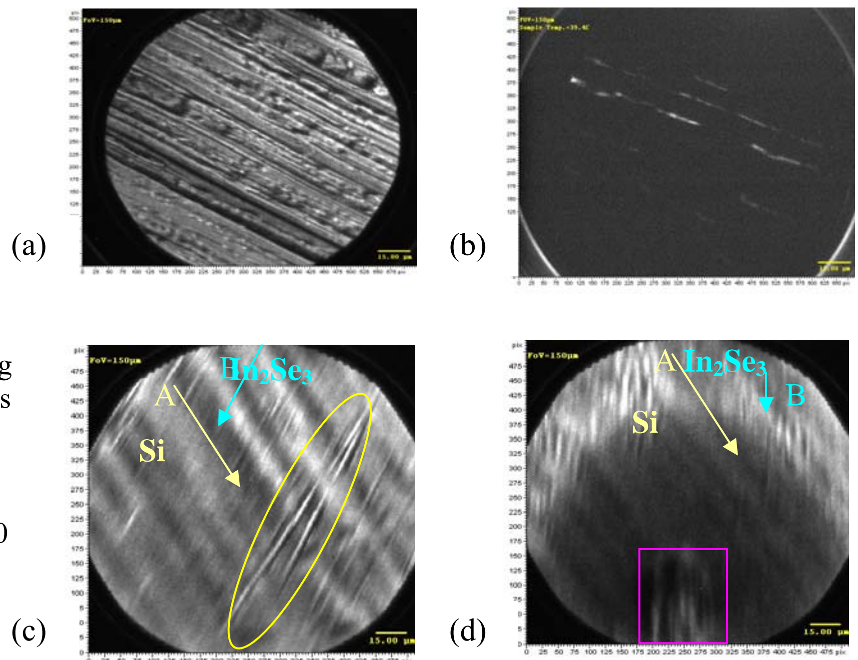

Figure 1. *PEEM images (field of view 150 μm, scale bar 30 μm) for (a) clean Si(111); (b) amorphous In_2Se_3 film on Si(111); (c) annealed In_2Se_3/Si(111); (d) after irradiation with 266-nm photon pulse. Images presented here are acquired with mercury lamp illumination (hv = 5.1 eV).*

photoelectron emission microscopy (PEEM), the crystallinity was probed with x-ray diffraction and low-energy electron diffraction, and the stoichiometry with Rutherford back-scattering spectroscopy. The stoichiometry, morphology, and crystal structure of the crystallized In_2Se_3 film and its orientation with respect to the substrate are determined.

The EMSL PEEM was equipped with both Hg (hν = 5.1 eV) and D_2 (hν = 6.0 eV) sources for imaging a 150-μm-diameter region of the sample. An Nd:YAG laser (λ = 266 nm, hν = 4.7 eV, FWHM pulse width 20 ns, spot diameter 100 μm, 0.1 mJ/pulse at 1 Hz repetition rate) was interfaced to the PEEM and used to amorphize the crystalline film. The laser is introduced through an ultraviolet-grade-fused silica window to the PEEM objective chamber holding the sample.

While a slow anneal below the melting temperature can lead to crystallization of an amorphous film, returning to the amorphous state requires rapid heating and cooling to quench in the disordered state. This was accomplished with pulsed laser annealing. The sample was monitored with the PEEM, which distinguishes structures on the surface through a combination of their work function, electrical conductivity, and density of states near the Fermi level.

Figure 1(a) shows a PEEM image of a clean Si(111) substrate after being argon-sputtered and then annealed around 850°C. An amorphous In_2Se_3/Si(111) film deposited is shown in Figure 1(b). The room-temperature-deposited In_2Se_3 film presents a completely dark PEEM image when using either the mercury lamp (5.1eV) or D_2 lamp (6.0 eV), except for defect lines running through the center of the image.

A PEEM image was obtained of the same film before [Figure 1(c)] and after [Figure 1(d)] laser annealing. Similar results were obtained with both mercury and D_2 illumination, although only the mercury results are shown. Comparison to silicon substrates without In_2Se_3 films [Figure 1(a)] indicates that the wider stripe structure running from upper left to lower right arises from the underlying silicon terrace structure (yellow arrows), while the narrower lines (blue arrows) correspond to the texture of the In_2Se_3 films. Two crossed lines marked in the oval are defects on the surface.

The 266-nm laser was used to anneal a spot on the sample approximately 150 microns in diameter near the place where the image in Figure 1(c) was taken., Single pulses of 0.1-mJ and 20-ns duration were measured at the laser head. Subsequent aperture-reduction and focusing culminated in a final pulse fluence of < 50 mJ/cm^2. The resulting annealed region is shown in Figure 1(d), where a dark circular region may be observed surrounded by features characteristic of the crystalline In_2Se_3 film. The darker region still shows (though with less contrast) the structure characteristic of the underlying silicon substrate, with In_2Se_3 features less distinct.

The contrast between the crystalline and amorphous regions in the PEEM could arise from differences in work function, in densities of states near the Fermi level, or in film conductivity. The work function of crystalline In_2Se_3 is 4.35eV, so both mercury (5.1 eV) and D_2 (6.0 eV) illumination should result in electron emission. Our photoemission measurements on a 1-nm-thick film show an In 4d core level shift of ~ 0.7 eV to higher binding energy (relative to the Fermi energy) from the amorphous to the annealed phase, while the silicon 2p shifts by only 0.1 eV in the same direction. If the In shift were completely due to a change in work function, then the mercury radiation would be close to threshold for photoemission, but there should still be significant emission with D_2 radiation. However, we find no emission with either source for the as-deposited film except at large-scale defects [Figure 1(b)]. It is thus likely that photoexcited electrons become trapped in the highly resistive amorphous material and cannot travel to the surface for emission into vacuum.

The control of material phase (amorphous, or one of several possible crystalline or polycrystalline states) is essential to the properties of modern devices. The difference in properties associated with a phase change may be exploited for device operations, as in DVDs where the change in optical reflectivity between crystalline and amorphous states allows media rendition. Driven by the need for a new paradigm to continue the relentless increase in both density and speed that has characterized developments in computer memory for four decades, one promising avenue for non-volatile memory is phase-change non-volatile memory, for which chalcogenides are prime candidates.

Amorphous-crystalline phase transitions can be achieved by applying voltage pulses with different amplitudes and durations in the range of tenths of nanoseconds. In our study, we have shown that rapid, selective, and local crystal-amorphous transformation can be realized using pulsed, ultraviolet nanosecond lasers at low fluences. This is a necessary step in the development of high-density/high-speed chalcogenides-based optical phase-change non-volatile memory.